Stochastic Modeling of Microwave Oven Interference in WLANs

Marcel Nassar
Dept. of Electrical and Comp. Eng.
The University of Texas at Austin
Email: nassar.marcel@mail.utexas.edu

Xintian Eddie Lin
Intel Corp.
Santa Clara, USA
Email: eddie.x.lin@intel.com

Brian L. Evans
Dept. of Electrical and Comp. Eng.
The University of Texas at Austin
Email: bevans@ece.utexas.edu

***Abstract*—An IEEE 802.11b/g/n wireless local area network (WLAN) experiences significant radio frequency interference (RFI) from microwave ovens, cordless phones, Bluetooth devices, and other WLANs operating in the 2.4 GHz band. In particular, microwave ovens emit interference that can either prevent an access point from transmitting or cause a dramatic increase in bit errors at the receiver. This paper investigates the disruption in delay sensitive streaming applications under microwave oven RFI. The proposed contributions of this paper include (1) a statistical-physical model of oven-generated RFI in WLAN channels that is dependent on distance and frequency, (2) an increase in the information rate bound of up to 5 bits/s/Hz due to the more realistic statistical-physical model of oven-generated RFI, and (3) a proposed transmission strategy to achieve the higher information rate bound.**

I. Introduction

IEEE 802.11b/g/n WLANs, operating in the 2.4GHz unlicensed Industrial, Scientific, and Medical (ISM) band, experience RFI from other ISM devices that operate with minimum regulation in the same band such as microwave ovens and Bluetooth devices. This leads to significant performance degradation [1]. In this paper, we focus our attention on microwave ovens and refer the interested reader to [1] and [2] for more information on other interference sources. Microwave ovens exhibit non-stationary statistics largely deviating from the Gaussian model and powers as high as -50dBm at 15m [2] (comparable to the transmit power of an access point (AP) in WLANs). This, compounded by a typical usage in the order of tens of minutes, leads to serious disruption for real-time streaming applications such as wireless video and presentations in home and office environments. Two general types of microwave ovens are in use: the"transformer-type" oven commonly used in households and the "inverter-type" oven generally used in commercial settings. These two types differ in the way they implement power transfer from the AC source to the magnetron that operates the microwave oven. In this work, due to space limitations we focus on transformer ovens and leave inverter ovens to future work. Fig. 1 shows the max-hold spectrum of the oven RFI. It is noticed that it is mainly concentrated in the $2.4-2.5$GHz range, the frequency range used by IEEE 802.11g/n. In fact, the transformer oven RFI has been shown to be a narrowband signal that sweeps through the 2.4GHz band [1], [3].

The effect of oven RFI on communication performance has been studied for IEEE 802.11b [4], [5] and for IEEE 802.11g systems [1], [6]. In [1], the authors propose a spectrum-sensing method to detect the presence of microwave oven emissions and adaptively change the MAC layer parameters to improve throughput. The mentioned papers employ various models of oven-generated RFI in their transmission strategy design and system-level simulations. One of the challenges in such simulations is how to model the oven-generated RFI. In particular, oven-generated RFI has a duration of tens of milliseconds, while the regular duration of an OFDM symbol in WLAN systems is on the order of microseconds. This large discrepancy in the durations, compounded with the limited memory of today's capture systems, prohibits in many cases the use of real oven interference data in system simulations. In addition, this approach does not yield any insight into the design of effective transmit strategies under RFI. Consequently, mathematical modeling of the oven-generated RFI is of great importance in system-level design.

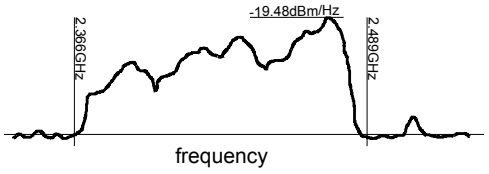

Fig. 1. Max-hold power spectral density of the transformer microwave oven indicates overlap of microwave emissions with the 2.4 GHz ISM band used for 802.11b/g/n wireless LANs. The oven's emission power is around 20dBm.

Previous work has modeled the oven RFI using deterministic equations or amplitude statistics. The deterministic approach models the oven RFI as an analytical function of time and frequency. The main deterministic model is the AM-FM model which is described in [4] and augmented for frequency drift in [3]. The main benefit of the AM-FM model is that it is able to capture the dependency of the oven-generated RFI on frequency. However, the deterministic nature of this model fails to model the randomness present in wireless channels. As the oven interference propagates through the wireless channel, it is subjected to various random channel impairments such as multipath, fading, and shadowing. In addition to that, the oven's emission patterns may change according to various conditions such as temperature, oven orientation, and oven loads [7]. These random aspects are captured well by using

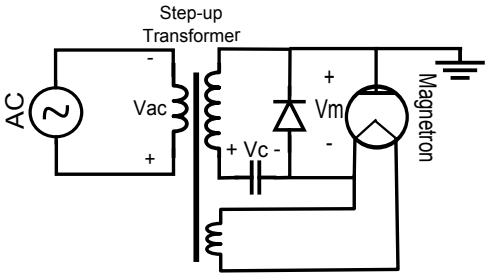

Fig. 2. Transformer microwave oven circuit diagram: during $V_{ac} > 0$, $V_m = 0$ and the magnetron is off, as soon as $V_{ac} < 0$ magnetron activates and emits radiation.

statistical models based on amplitude statistics of oven RFI such as the Gaussian mixture model [6] and the Middleton class-A model [8]. However, these models fail to capture the effect of frequency (the selected WLAN channel) on the interference properties. In particular, they assume that the oven RFI is present in all channels simultaneously for the whole duration of magnetron activity and then it disappears during the magnetron inactivity period; hence we refer to these models as High-Low models. We will show that these models often lead to pessimistic estimates of communication performance under oven RFI and to conservative designs which may fail to meet throughput requirements.

In this paper, we propose a stochastic model that will bridge the gap between the deterministic and statistical models. Contrary to the used High-Low model, our proposed model is based on the amplitude statistics of the oven RFI and reflects the dependence on the distance and the frequency-band of the WLAN channel under consideration. We validate the model using oven measurements and show its improved accuracy over the High-Low model in modeling oven RFI measurements. Then, we investigate the maximum information rates supported by the oven RFI additive channel and propose different strategies to maximize available data rates.

II. Microwave Oven's Operation

This section explains the physical operation of transformer ovens on which we base our proposed model in Section IV. The basic circuit diagram of such an oven is given in Fig. 2 [9]. The AC power source is stepped up to around 2kV through the transformer. The positive half cycle of the AC voltage source V_{ac} charges the capacitor through the conducting diode. During this time, the voltage across the magnetron (V_m) is reduced to zero because the diode forms a closed switch. As the voltage V_{ac} turns negative, the diode becomes an open circuit and the capacitor starts to discharge and adds to the second winding voltage to produce double the voltage (around 4kV) at the magnetron input ($V_m = V_c + |V_{ac}|$). The capacitor's main function is converting the AC source into a high voltage DC source required to excite the magnetron into emitting electromagnetic waves that heat up the food. As a result, the voltage across the magnetron (V_m), and thereby the microwave emission, will be on during the positive half of the duty cycle of the AC source (V_{ac}) and off during the negative part and the wireless transceiver will experience oven-generated RFI only during half of the AC cycle ($\frac{1}{2}\frac{1}{60Hz} = 8.3$ms in the US). Due to the periodicity of the AC source, the interference will repeat with the same frequency f_{AC} as the source.

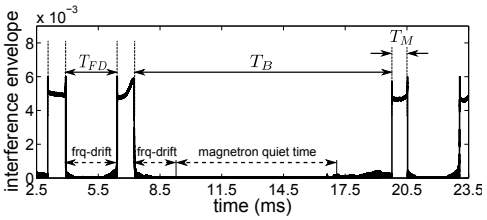

Fig. 3. Oven RFI in channel 11 (magnitude of I-Q samples at 3m distance). The effect of magnetron frequency drift can be seen from the parameter T_{FD}.

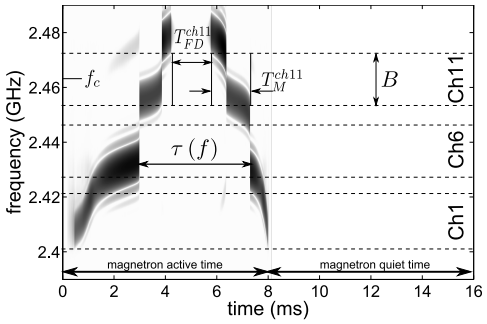

Fig. 4. Spectrogram of oven RFI in the 2.4GHz band. This shows how the T_{FD} and T_M parameters for channel 11 relate to the same parameters in Fig. 3.

III. Temporal and Spectral Characterization

A. Measurement Setup

The measurements were collected using a laptop antenna, at a distance of 3m, connected to a downconverter chain followed by a digitizer board sampling at 200Msample/sec with 14bits/sample accuracy. The measurements were equalized to account for the downconverter-digitizer path transfer function.

B. Results

The time-domain envelope of oven RFI in channel 11 (IEEE802.11g, 20MHz, $f_c = 2.462$GHz), shown in Fig. 3, confirms the 8ms high-interference and 8ms low-interference structure expected from the discussion in Section II. However, there seems to be a time period during the high-interference state where the interference is greatly reduced in magnitude. A more detailed picture is given by the spectrogram in Fig. 4 which plots the oven RFI in the 2.4-2.5GHz range. The transformer oven interference is narrowband and sweeps the whole 2.4-2.5GHz range. This is due to the frequency-drift phenomenon whereby the magnetron oscillation frequency varies with the applied voltage V_m [3]. Thus, observing a given frequency band will show the oven RFI appearing and disappearing according to the drift in the magnetron frequency as shown in Fig. 4 and Fig. 3. Our model will capture the dependence between the oven RFI and the observed frequency band, which the High-Low model fails to do.

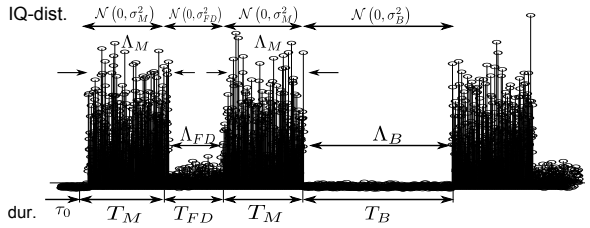

Fig. 5. Envelope of the proposed microwave oven model. It is divided into three main states: S_B,S_M, and S_{FD} based on the properties of the channel 11 trace in Fig.3.

TABLE I
SUMMARY OF THE MODEL'S MAIN PARAMETERS

Parameter	Value
σ_B^2	$N_0 B$
$\sigma_M^2(d)$	$\Gamma(d)+\sigma_B^2$
$\sigma_{FD}^2(d)$	$\Gamma_{ch}\Gamma(d)+\sigma_B^2$
$T_{FD}(f_c,B)$	Eq. (3) $\approx \alpha_1 f_c + (\alpha_1 B/2 + \alpha_0)$
$T_M(f_c,B)$	Eq. (3) $\approx \lvert\alpha_1 B\rvert$
$T_B(f_c,B,f_{AC})$	$f_{AC}^{-1} - 2T_M(f_c,B) - T_{FD}(f_c,B)$

IV. STOCHASTIC MODEL OF OVEN-GENERATED RFI

In this paper, we extend the High-Low model used in [6] to incorporate two important aspects of oven RFI: 1) dependency on the distance separating the oven from the transceiver and 2) the dependency on the frequency band of the WLAN channel. The proposed model is depicted in Fig. 5 and given analytically by

$$z[n] \sim \begin{cases} \mathcal{N}_c\left(0,\sigma_M^2\right) & \text{if } (nT_s-\tau_0)_T \in \Lambda_M, \\ \mathcal{N}_c\left(0,\sigma_{FD}^2\right) & \text{if } (nT_s-\tau_0)_T \in \Lambda_{FD}, \\ \mathcal{N}_c\left(0,\sigma_B^2\right) & \text{if } (nT_s-\tau_0)_T \in \Lambda_B \end{cases} \quad (1)$$

where $z[n]$ is the complex-baseband noise sample, T_s is the sampling period, $(.)_T$ represents the modulo operation, and $\tau_0 \sim \mathrm{U}[0,T]$ is random offset time. The model is periodic with period $T = f_{AC}^{-1} = T_B + 2T_M + T_{FD} \approx 16.7$ms and time intervals $\{\Lambda_i\}_{i\in\{M,B,FD\}}$ are specified in Fig. 5. During each period, the time trace is divided into three states each corresponding to AWGN channels with different variances (see Fig. 5). In particular, the states $S_B(T_B,\sigma_B^2)$, $S_M(T_M,\sigma_M^2)$, and $S_{FD}(T_{FD},\sigma_{FD}^2)$ represent the states when there is only background noise, when the oven RFI is present in the channel, and during the time when the magnetron frequency is outside of the specified frequency band respectively. In general, $\sigma_{FD}^2 \approx \sigma_B^2 \ll \sigma_M^2$ (See Fig. 3). As a result, the model can be simplified to a two state model (S_B and S_M) where S_B becomes of duration $T_B + T_{FD}$.

A. Dependence on Distance

Oven RFI propagates through the wireless medium. As a result, the power of this interference will follow the exponential decay specified by pathloss models. On top of that, the oven RFI is subjected to the same wireless channel impairments (multipath, fading and shadowing) as a narrowband signal. This fact justifies modeling the oven RFI as a complex Gaussian variable (as done in the previous paragraph). Since we are interested in analyzing the effect of microwave ovens on WLANs, we employ the propagation models used in the IEEE802.11n standard. σ_B^2 is the variance of the thermal background noise in receiver electronics and thus is independent of the distance between the oven and transceiver. On the other hand, σ_M^2, the variance of the noise during the on-state of the magnetron, is the superposition of thermal noise and oven transmit power. Thus, it is distance dependent and can be written as $\sigma_M^2(d) = \Gamma(d) + \sigma_B^2$ where $\Gamma(d) = P(d) = \frac{P_0}{L_p(d)}$. P_0 and $P(d)$ represent the microwave oven transmit power and power at distance d respectively. $L_p(d)$ is the pathloss experienced by the oven RFI, and is specified by the IEEE802.11n propagation model [10] as

$$L_p(d) = \begin{cases} L_{FS}(d) & d \le d_{BP} \\ L_{FS}(d_{BP}) + 10\log\left(\frac{d}{d_{BP}}\right)^{\eta} & d > d_{BP} \end{cases} \quad (2)$$

where η and d_{BP} are the pathloss exponent and breakpoint distance respectively, and $L_{FS}(d) = 10\log\left(\frac{4\pi d}{\lambda}\right)^2$ is the free-space path loss. The variance of the interference corresponding to the magnetron frequency-drift is given by $\sigma_{FD}^2 = \Gamma_{ch}\Gamma(d) + \sigma_B^2$ where Γ_{ch} is a channel specific multiplier. When $\Gamma_{ch}\Gamma(d) \ll \sigma_B^2$, then $\sigma_{FD}^2 = \sigma_B^2$ and states S_{FD} and S_B become indistinguishable.

B. Dependence on Frequency

WLANs divide their available bandwidth into multiple channels of bandwidth B. Observing Fig. 4, it appears that the interference power is spread across the channels almost uniformly. However, the temporal properties of the interference are considerably different. In particular, observing zero-bandwidth band at frequency f shows the oven RFI appearing and then disappearing at a certain time t only to reappear at time $t+\tau(f)$. We will refer to the time $\tau(f)$ as the inter-arrival time of the oven RFI. On top of that, Fig. 4 shows how the parameters of Fig.3 relate to $\tau(f)$. As a result, it can be seen that different WLAN channels will have distinct temporal parameters T_M, T_{FD} and T_B given by

$$\begin{aligned} T_{FD} &= \tau\left(f_c + \frac{B}{2}\right) \\ T_M &= \frac{1}{2}\left(\tau\left(f_c - \frac{B}{2}\right) - \tau\left(f_c + \frac{B}{2}\right)\right) \\ T_B &= f_{AC}^{-1} - 2T_M - T_{FD} \end{aligned} \quad (3)$$

where f_c is the center frequency of the channel under consideration. The model parameters are summarized in Table I, while their estimation from measured data is discussed in Section V.

V. STATISTICAL FITTING AND MODEL VALIDATION

This section discusses the parameter estimation and the accuracy of the proposed model when used to fit actual interference data.

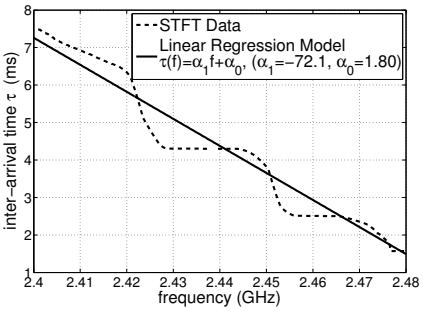

Fig. 6. Estimation of $\tau(f)$ using short-time Fourier transform in Eq. (4) and a linear regression model in Eq. (5).

A. Temporal Parameter Estimation and Fitting

The estimation of parameters T_M, T_{FD}, and T_B involves the computation of the inter-arrival time $\tau(f)$ at particular frequencies (see (3)). Toward this end, we compute a narrowband short-time Fourier transform (smaller window size increases temporal resolution) of the oven RFI for the duration of one period (16.6ms). Let $X(n, f_0)$ be the short-time Fourier transform (STFT) at frequency f_0. The inter-arrival time $\tau(f_0)$ is approximated by

$$\hat{\tau}(f_0) = |n_1 - n_2| \times T_S \tag{4}$$

where T_S is the sampling period and n_1, n_2 are the time-indices of the first peak and the second peak of the amplitude of $X(n, f_0)$. A simpler approach is to model the relation between the frequency and inter-arrival times as linear. Then the result of computing $\hat{\tau}(f)$, defined in (4), at 512 frequency values is fitted to the following linear regression model

$$\hat{\tau}(f) = \alpha_1 f + \alpha_0. \tag{5}$$

The inter-arrival times computed by both methods are given in Fig. 6. Table II shows how well our estimators perform in predicting T_B and T_M for IEEE802.11g/n channels 1,6, and 11 (these channels approximately partition the IEEE802.11g spectrum). This table compares the actual value of the parameters, obtained by examining the time trace of the corresponding channels, to the estimates obtained by (3) and estimating τ using the STFT and linear regression in (4) and (5). It is noticed that the produced estimates provide a good estimate for the given parameters, with the STFT-based approximation being more accurate. However, the linear model is more easily applied to approximate the temporal parameters because it does not require the trace of the data. In general, the linear regression model may lead to some over-approximation in T_M which will result in an upper-bound on communication performance but is considerably more accurate than the High-Low model.

B. Statistical Models

This section introduces the statistical models used to fit oven RFI. These models characterize the first-order pdf of the complex-baseband noise samples (I and Q) obtained by the receiver in a specific IEEE802.11g/n channel.

TABLE II
FITTING OF THE TEMPORAL PARAMETERS

		Actual Value	τ **(STFT)**	τ **(Linear)**
Ch1	T_M	1.00ms	1.65ms	1.44ms
2.412GHz	T_{FD}	6.50ms	5.77ms	5.67ms
Ch6	T_M	1.40ms	1.44ms	1.44ms
2.437GHz	T_{FD}	4.30ms	4.16ms	3.87ms
Ch11	T_M	0.87ms	0.85ms	1.44ms
2.462GHz	T_{FD}	2.50ms	2.26ms	2.06ms

1) Gaussian Mixture Distribution: Gaussian Mixture distributions extend the structure of normal distributions to model complex real-life data. This structure is constructed using a linear superposition of normal distributions. In particular, a N-term Gaussian Mixture distribution consists of a set of complex normal distributions $\left\{\mathcal{N}_c\left(\mu_i, \sigma_i^2\right)\right\}_{i=1}^{N}$ and a normalized mixing vector $\pi = [\pi_1 \pi_2 \cdots \pi_N]$. The mixing vector π can be interpreted as following: let x be a realization of a random variable drawn from a Gaussian mixture distribution, then $\pi_i = \Pr\left[x \sim \mathcal{N}_c\left(\mu_i, \sigma_i^2\right)\right]$; i.e, π is the discrete probability density of a latent variable S that determines from which distribution is a given sample drawn from. Then the pdf of the Gaussian Mixture is given by the sum of the N complex normal distribution weighted by the mixing vector. The pdf of the N-term Gaussian mixture is given by

$$f(x) = \sum_{i=1}^{N} \pi_i \cdot \mathcal{N}_c\left(x; \mu_i, \sigma_i^2\right). \tag{6}$$

The parameters of this model were estimated using the EM-algorithm [11].

2) Middleton Class-A Distribution: Middleton Class-A distribution is a statistical-physical model used to model impulsive narrowband noise produced by a Poisson field of interferers [12]. This model has been used to model microwave oven interference in [8] and [5]. The Middleton Class-A distribution is characterized by the following parameters: an overlap index A, a power ratio Γ_A, its variance σ^2, and its mean μ. The class-A model is a special case of the Gaussian mixture model with $N \to \infty$, $\pi_m = e^{-A}\frac{A^m}{m!}$, and $\sigma_m^2 = \sigma^2 \cdot \frac{m/A + \Gamma_A}{1+\Gamma_A}$. Parameter estimation was performed by the Method of Moments [12].

C. Statistical Properties of the Proposed Model

We now proceed to derive the first-order statistics for the proposed model using the states S_M, S_B, and S_{FD} defined in Section IV. Let X be a random variable with the first-order distribution[1] of the proposed model, then the pdf of X conditioned on the channel state $S \in \{S_M, S_B, S_{FD}\}$ is given by $f_{X|S}(x|s) = \mathcal{N}_c\left(x; \mu_s, \sigma_s^2\right)$. Now using the law of total probability, the first-order density of the random variable X is given by

$$f_X(x) = \sum_{s \in \{S_H, S_I, S_L\}} \Pr[s]\, \mathcal{N}_c\left(x; 0, \sigma_s^2\right) \tag{7}$$

[1]Since we are fitting first-order pdfs all temporal correlations are ignored and samples are treated as independent and identically distributed (iid).

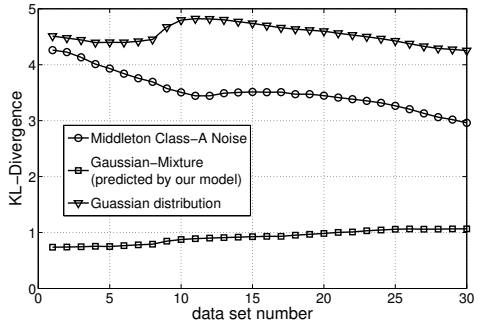

Fig. 7. The fitting of complex-baseband statistics of oven RFI in channel 11 at a distance of 3m. The statistics predicted by our model provide the best fit.

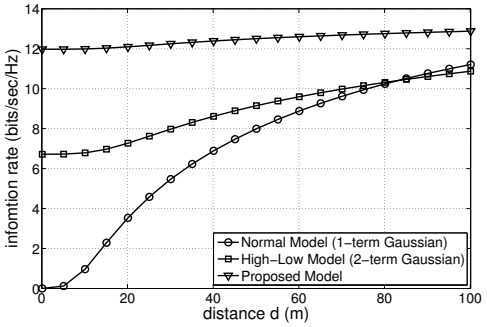

Fig. 8. Gain in information rate due to more accurate modeling (ch.11 parameters with $T_M = 0.87$ms and $T_{FD} = 2.5$ms, oven transmit power of 20dBm, and $SNR = \frac{E_r}{\sigma_B^2} = 40$dB).

which is the Gaussian mixture model with $\pi_s = \Pr[s]$. Using the frequency interpretation of probability, it is observed that $\Pr[S_B] = \frac{T_B}{T_B+T_{FD}+2T_M}$, $\Pr[S_{FD}] = \frac{T_{FD}}{T_B+T_{FD}+2T_M}$, and $\Pr[S_M] = \frac{2T_M}{T_B+T_{FD}+2T_M}$.

D. Model Fitting and Validation

In order to verify the validity of the proposed model, we fit collected microwave oven data of channel 11 (used in Section III) to the models discussed in Section V-B. The KL-divergence, $D_{KL}(P_e \| P_M)$ where P_e is the empirical distribution and P_M is the model distribution, is used to quantify the fit to the empirical data. The fit is given in Fig. 7. It is seen that the distribution predicted by our model provides the best fit when compared to a normal distribution and the class-A distribution (used in [5], [8]). This can be explained by the fact that class-A model was derived based on the assumption that there is a Poisson field of interferers [12], which is not the case when the interference is resulting from the operation of a single microwave oven.

VI. Communication Performance of WLANs under Microwave Oven Interference

Microwave ovens degrade the throughput performance of WLANs [1], [6]. Different strategies such as avoidance [13], rate adaptation [6], and MAC layer parameter optimization [1] have been proposed to sustain an acceptable throughput performance in WLANs. The performance benefit of these strategies is studied by system simulation. As a result, it is important to use an accurate simulation model of microwave oven interference in order to get a reasonable estimate of system's throughput under real microwave oven interference. On top of that, an accurate interference model provides valuable insight into the design of transmitter strategies and the optimization of their parameters. This section addresses both of these issues from an information theoretic perspective.

A. Information Rate Increase due to more Accurate Modeling

As discussed in Section I, there are various interference models used to study the performance of WLANs under oven RFI. In this section, we investigate the effect of modeling on the predicted information rate of channels corrupted by oven RFI. We assume that there is no power allocation being done. In particular, we will compare our model to the High-Low model used in [1] and [6]. On top, both models are compared to the case where the oven RFI is assumed to be a white Gaussian process. We assume that the transmitter has perfect channel state information (CSI) represented by the channel noise variance σ_S^2 where $S \in \Omega = \{S_M, S_B, S_{FD}\}$. This assumption is justified in practice since the symbol period in WLANs is much lower than the duration of a specific state of the oven RFI thereby allowing for sufficient time for feedback from the receiver (the symbol time is $4\mu s$ while the duration of a state in the oven interference is in the order of milliseconds). Given the CSI, the channel looks like an AWGN channel with variance σ_S^2. As a result, the information rate of the channel under our model without power allocation is given by

$$I_{CSI} = \mathbf{E}_S\left[\log\left(1+\frac{E_r}{\sigma_S^2}\right)\right] = \sum_{s\in\Omega}\pi_s \log\left(1+\frac{E_r}{\sigma_s^2}\right) \quad (8)$$

where the E_r is the energy of the received signal, π_s and σ_s^2 are parameters defined in Section V-C. On the other hand, the information rate of the High-Low model is given by the same formula with the state S being restricted to $\{S_M, S_B\}$ and taking those states with probability $1/2$. The rate in the case where the oven RFI is assumed to be a Gaussian process is given by

$$I_{CSI}^G = \log\left(1+\frac{E_r}{\mathbf{E}_S[\sigma_S^2]}\right) \quad (9)$$

where $\mathbf{E}_S[\sigma_S^2] = \sum_{s\in\Omega}\pi_s\sigma_s^2$. Fig. 8 illustrates the information rate loss (around 4bits/s/Hz at 20m) due to inaccurately modeling the oven RFI as the High-Low model rather than our proposed model that is based on the physical properties of the oven RFI. In this figure, the High-Low model was augmented to account for distance by viewing it as a special case of our proposed model when frequency dependence is ignored ($T_{FD} = 0$ms) with $T_M = 4$ms and $T_B = 8$ms. This rate loss is due to the assumption that every WLAN channel is subjected to the full oven RFI while Fig. 4 clearly suggests otherwise. The information rate under the Gaussian assumptions is the

lowest. This is expected since it ignores the temporal structure of the noise.

B. Information Rate and Transmission Strategies

In this section, we investigate the information rate of various transmission strategies in channels corrupted by oven RFI under the availability of transmit CSI and no power allocation. Fig. 9 shows the information rate of various transmission strategies and compares them to the case with no oven RFI. There are two avoidance strategies that send data only when there is no oven RFI present. The maximum information rate of these avoidance strategies is given by the mutual information between the channel input and output. This mutual information is given by

$$I\left(x,y|S\right)=\frac{T_x}{T}\log\left(1+\frac{E_r}{\sigma_B^2}\right) \tag{10}$$

where T_x is the time that the avoidance strategy transmits, and T is the total time available for transmission. The blind strategy assumes the High-Low model and thus transmits only at half the rate of the channel capacity with no oven interference (since $T_x = 8$ms and $T = 16$ms) [13]. However, our proposed model-aware avoidance strategy that is based on our model's temporal properties ($T_x = T_B + T_{FD} \approx 14$ms and $T = 16$ms) results in a 5bits/s/Hz increase in transmission rate since it takes into account the fact that the interference seen by each WLAN channel is much shorter. It should be noted that the transmission rate of both the avoidance strategies does not scale with distance as opposed to the actual capacity of the microwave oven channel. This is due to the fact that the avoidance strategies send information only during the time when the background noise (σ_B^2), which is independent of the distance, is present. The capacity, on the other hand, increases with the distance between the oven and the receiver due to the fact that the oven RFI power is reduced due to pathloss as expressed by parameters $\sigma_M^2\left(d\right)$ and $\sigma_{FD}^2\left(d\right)$. However, this increase is slow at smaller distances ($d < 20$m like in small apartments) which indicates that a model-aware avoidance strategy is almost optimal and should be preferred due to its lower implementation complexity. At higher distances ($d > 20$m like in houses, offices, universities and malls) the capacity of the channel increases and deviates from the avoidance strategy. This can be interpreted by the fact that at those distances it is advantageous to transmit even during the period when the oven is active. The intuition is that at such distances the interference is reduced to a level where additional information can be sent over the channel during that period. This suggests that adaptive-modulation can be used to increase the data rates in the presence of the oven interference.

VII. Conclusion

This paper proposes a general stochastic model for transformer microwave ovens based on their circuit-level operation. Previous models are extended by including dependence on the frequency band of the WLAN channel and the distance between the oven and the receiver. After that, the actual information rate that can be supported by the channel is shown to be higher than predicted by previous models. This is utilized to propose various rate-increasing transmission strategies such as model-aware avoidance transmission at smaller distances and adaptive modulation at larger distance.

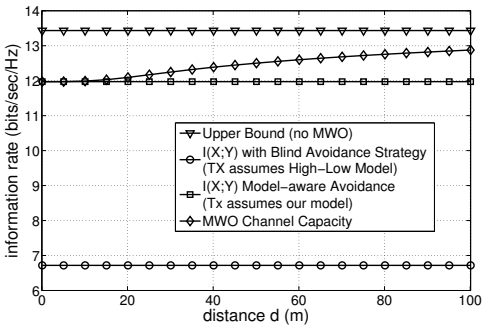

Fig. 9. Maximum information rate of different strategies vs. distance in the microwave oven (MWO) channel (same parameters as in Fig. 8).

Acknowledgement

The authors would like to thank Mr. Omar El Ayach for his helpful comments and discussions. M. Nassar and B.L. Evans were supported by research funding and an equipment gift by Intel Corporation during this research.

References

[1] S. Srikanteswara and C. Maciocco, "Interference mitigation using spectrum sensing," in *Proc. Int. Conf. Comp. Comm. & Net.*, 2007, pp. 39–44.

[2] K. Blackard, T. Rappaport, and C. Bostian, "Measurements and models of radio frequency impulsive noise for indoor wireless communications," *IEEE Journal Select. Areas in Comm.*, vol. 11, pp. 991–1001, 1993.

[3] Y. Zhao, B. Agee, and J. Reed, "Simulation and measurement of microwave oven leakage for 802.11 WLAN interference management," in *Proc. IEEE Int. Symp. on Microwave, Antenna, Propagation and EMC Technologies for Wireless Comm.*, vol. 2, 2005, pp. 1580–1583 Vol. 2.

[4] Y. Matsumoto, M. Takeuchi, K. Fujii, A. Sugiura, and Y. Yamanaka, "Performance analysis of interference problems involving DS-SS WLAN systems and microwave ovens," *IEEE Trans. Electromagn. Compat.*, vol. 47, no. 1, pp. 45–53, 2005.

[5] S. Miyamoto and N. Morinaga, "Effect of microwave oven interference on the performance of digital radio communications systems," in *Proc. IEEE Int. Conf. on Comm.*, vol. 1, 1997, pp. 51–55.

[6] S. Miyamoto, S. Harada, and N. Morinaga, "Performance of 2.4 GHz-band wireless LAN system using orthogonal frequency division multiplexing scheme under microwave oven noise environment," in *Proc. IEEE Int. Symp. on Electromagn. Compat.*, vol. 1, 2005, pp. 157–162.

[7] P. Gawthrop, F. Sanders, K. Nebbia, and J. Sell, "Radio spectrum measurements of individual microwave ovens vol.1," NTIA, Tech. Rep. 94-303-1, March 1994.

[8] H. Kanemoto, S. Miyamoto, and N. Morinaga, "Statistical model of microwave oven interference and optimum reception," in *IEEE Int. Conf. on Comm.*, vol. 3, 1998, pp. 1660–1664.

[9] H. Kako, T. Nakagawa, and R. Narita, "Development of compact inverter power supply for microwave oven," *IEEE Trans. Consum. Electron.*, vol. 37, no. 3, pp. 611–616, Aug. 1991.

[10] E. Perahia, *Next Generation Wireless LANs : Throughput, Robustness, and Reliability in 802.11n*. Cambridge University Press, 2008.

[11] C. M. Bishop, *Pattern Recognition and Machine Learning*, 2006.

[12] D. Middleton, "Procedures for determining the parameters of the first-order canonical models of class A and class B electromagnetic interference," *IEEE Trans. Electromagn. Compat.*, no. 3, pp. 190–208, 1979.

[13] T. Taher, M. Misurac, J. LoCicero, and D. Ucci, "Microwave oven signal interference mitigation for Wi-Fi communication systems," in *Proc. IEEE Consum. Comm. and Net. Conf.*, 2008, pp. 67–68.